ACCOUNTS
of chemical research

Covalent Electron Transfer Chemistry of Graphene with Diazonium Salts

GERALDINE L. C. PAULUS,† QING HUA WANG,† AND MICHAEL S. STRANO*

Department of Chemical Engineering, Massachusetts Institute of Technology, Cambridge, Massachusetts 02139, United States

RECEIVED ON MAY 7, 2012

CONSPECTUS

Graphene is an atomically thin, two-dimensional allotrope of carbon with exceptionally high carrier mobilities, thermal conductivity, and mechanical strength. From a chemist's perspective, graphene can be regarded as a large polycyclic aromatic molecule and as a surface without a bulk contribution. Consequently, chemistries typically performed on organic molecules and surfaces have been used as starting points for the chemical functionalization of graphene. The motivations for chemical modification of graphene include changing its doping level, opening an electronic band gap, charge storage, chemical and biological sensing, making new composite materials, and the scale-up of solution-processable graphene.

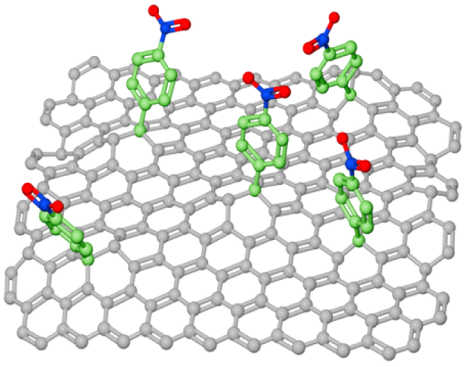

In this Account, we focus on graphene functionalization via electron transfer chemistries, in particular via reactions with aryl diazonium salts. Because electron transfer chemistries depend on the Fermi energy of graphene and the density of states of the reagents, the resulting reaction rate depends on the number of graphene layers, edge states, defects, atomic structure, and the electrostatic environment. We limit our Account to focus on pristine graphene over graphene oxide, because free electrons in the latter are already bound to oxygen-containing functionalities and the resulting chemistries are dominated by localized reactivity and defects. We describe the reaction mechanism of diazonium functionalization of graphene and show that the reaction conditions determine the relative degrees of chemisorption and physisorption, which allows for controlled modulation of the electronic properties of graphene. Finally we discuss different applications for graphene modified by this chemistry, including as an additive in polymer matrices, as biosensors when coupled with cells and biomolecules, and as catalysts when combined with nanoparticles.

Introduction

Single layer graphene (SLG) is a planar sheet of sp^2-bonded carbon atoms arranged in a hexagonal crystal lattice with remarkable electronic, physical, and chemical properties.[1] The π-orbitals in graphene are delocalized throughout the structure such that all conjugated chemical bonds are equivalent. Recently, significant efforts have focused on covalently functionalizing graphene to achieve band gap tuning and modulation of its doping level for various (opto-)electronic and sensing applications and for interfacing graphene with other materials.[2−5] In contrast to noncovalent functionalization, covalent schemes are more robust and change the electronic properties more strongly due to disruption of the crystallographic lattice.[5] The stability of the extended delocalized π-system ensures that the basal plane of graphene is fairly chemically stable. It is therefore not surprising that much work on graphene functionalization has been accomplished using highly reactive aryl radicals.

In this Account, we review the work from our laboratory[6−10] and others[3,11−21] on the covalent functionalization of graphene with aryl diazonium salts, which react via an electron transfer mechanism. We describe the reaction mechanism of the widely used diazonium functionalization of graphene, the effect of physical structure and supporting substrate on the reactivity of graphene, the effect of the functionalization on the electronic transport in devices, and its use in building complex chemical structures and sensors.

10.1021/ar300119z

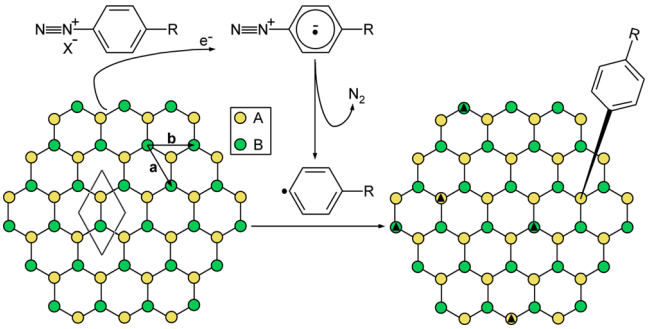

FIGURE 1. Schematic illustration of grafting a diazonium salt with functional group R and counterion X^- to a graphene sheet. Two carbon atoms (in the A and B sublattices) make up the unit cell (gray diamond) of the graphene sheet (with lattice vectors **a** and **b**). Thermodynamically favored lattice positions for further functionalization are marked with black triangles.

Reactions with Aryl Diazonium Salts

Diazonium salts with many different functional groups have been successfully grafted to graphene, including 4-nitrobenzene diazonium tetrafluoroborate (4-NBD),[7,8,10,11,14,16,17,21] 4-bromobenzene tetrafluoroborate (4-BBD),[7,18,20] 4-propargyloxybenzene diazonium tetrafluoroborate (4-PBD),[6,7] and 4-*tert*-butylphenyldiazonium tetrafluoroborate (4-TBD).[19]

Reaction Mechanism: Theory and Experiment. The most common reaction mechanism of covalent functionalization with aryl diazonium salts is illustrated in Figure 1. A delocalized electron is transferred from the graphene to the aryl diazonium cation, which becomes an aryl radical after releasing a molecule of N_2. The aryl radical then forms a covalent bond with a carbon atom in the graphene lattice, changing its hybridization to sp^3 and displacing it out of the plane by ~0.7 Å.[22] The attachment of a phenyl group results in a delocalized, unpaired electron. Density functional theory (DFT) calculations have shown that a second aryl group preferentially attacks at the para-position, also known as (1,4)-functionalization.[22] Pairwise additions in the A and B sublattices are thermodynamically favorable, and for small adsorbates such as hydrogen atoms, the theoretical maximum coverage is 25% for an areal concentration of $\sim 9 \times 10^{14}/cm^2$.[23] However for phenyl groups, Jiang et al. calculate a maximum packing of only 11% coverage ($\sim 4 \times 10^{14}/cm^2$), attributed to steric hindrance, still in a (1,4)-configuration (Figure 1).[22] These theoretical simulations predicting long-range ordering are based on the thermodynamics of the reaction. However, since the aryl radical is so reactive, the activation energy for the reaction is very low and the reaction is likely dominated by kinetics rather than thermodynamics, preventing any long-range ordering.[3] Quite surprisingly there does exist some experimental evidence of long-range ordering in selected area electron diffraction pattern (SAED) data of functionalized graphene,[24] although the observed pattern deviates from the theoretically predicted (1,4)-functionalization. It is very likely that the reaction conditions determine whether one operates in the thermodynamic or the kinetic regime. Throughout this Account, we will elaborate on the effects of the reaction conditions.

Experimentally, different concentrations of covalently bound species have been reported: 25% by using cyclic voltammetry (CV),[11] 12.5% by SAED,[24] 5% by scanning tunneling microscopy and spectroscopy (STM/STS),[16] 13% and 1.2% by a thermogravimetric analysis coupled to mass spectroscopy (TGA/MS),[19] and 0.3% based on Raman spectroscopy.[10] Rather than concluding that these results are contradictory, we argue that the reported values strongly depend on the reaction conditions and the conditions at which the measurements are taken.

Under some reaction conditions, physisorption of aryl molecules is promoted rather than (or in addition to) chemisorption. Englert and co-workers show with TGA/MS that 4-TBD functionalized graphene loses mass in two steps: at ~210 °C due to the desorption of physisorbed molecules and at ~480 °C due to cleavage of covalently bound molecules.[19] Hossain et al. report STM images of epitaxial graphene functionalized with 4-NBD showing chain-like features, suggestive of aryl oligomers.[16] The physisorbed portion of the oligomers inhibits further covalent attachment.[16] Atomic force microscopy (AFM) measurements also suggest multilayer formation.[17,24] Farmer et al. use milder reactions conditions than most others (1 mM of 4-BBD in a 1:1 mixture of water and methanol for 2 h at room temperature) and do not observe a significant increase of the D peak in their Raman spectra but do observe other Raman changes indicative of doping via physisorption.[20] Koehler et al. explicitly demonstrate how Raman spectroscopy can distinguish between physi- and chemisorption by exposing SLG to a concentrated 4-NBD solution (ensuring chemisorption) as well as to pure nitrobenzene, which lacks the diazonium group for covalent attachment (thereby ensuring physisorption).[17] In the first case, they observe a strongly increased value of the D to G integrated peak intensity ratio (I_D/I_G), whereas for the latter case, they detect an upshift of the G-peak position and a decrease of the 2D/G intensity ratio (I_{2D}/I_G), both indicative of doping.[25] Under many reaction conditions, a combination of both covalent binding or chemisorption (increased I_D/I_G) and noncovalent doping or physisorption (shifts in the G and 2D peak, as well as an decreased I_{2D}/I_G) is present.[7,10]

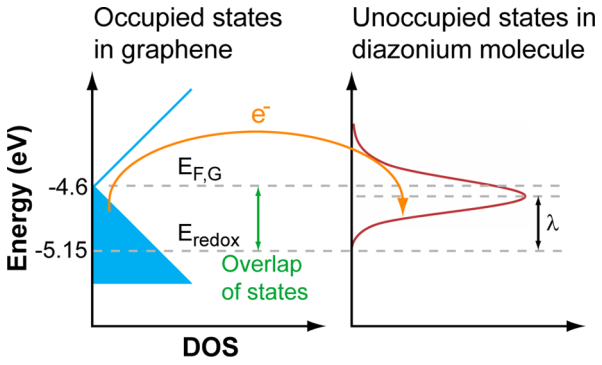

FIGURE 2. Schematic representation of the graphene DOS and the unoccupied DOS of a typical diazonium salt.

Reaction Rate. The rate-limiting step in the reaction of diazonium salts with graphene is the reduction of the diazonium salt by graphene to form the aryl radical. The reaction rate constant is determined from the theory of electron transfer reactions at electrodes,[26] and has been applied by our group to describe diazonium functionalization of single-walled carbon nanotubes (SWNTs)[27] and graphene.[8−10] The rate is determined by the overlap between the electronic density of states (DOS) of the graphene and the diazonium reactants in solution, as illustrated in Figure 2. Electron transfer occurs between any occupied state of the graphene that is matched in energy with an unoccupied state of the diazonium. The electron transfer rate constant, k_{ET}, is

$$k_{ET} = \nu \int_{E_{redox}}^{E_{F,G}} \varepsilon_{red}(E)\mathrm{DOS}_G(E)W_{ox}(\lambda, E)\, dE \qquad (1)$$

where

$$W_{ox}(\lambda, E) = \frac{1}{\sqrt{4\pi\lambda kT}} \exp\left(-\frac{(E - (E_{redox} + \lambda))^2}{4\lambda kT} \right) \qquad (2)$$

is the probability density function of vacant states in the diazonium molecule, ν is the electron-transfer frequency, ε_{red} is a proportionality factor, and DOS_G is the density of states of graphene. The term λ is the energy difference between the standard potential for the redox couple of the diazonium salt (E_{redox}) and the energy for maximum probability of finding a vacant state in the diazonium and has a value of 0.5−1 eV.[26] E_F is the Fermi energy (−4.6 eV for undoped graphene),[28] k is the Boltzmann constant, and T is absolute temperature. The redox potential for different diazonium salts can be determined via polarography: with respect to vacuum, $E_{redox,4\text{-NBD}} = -5.15$ eV and $E_{redox,4\text{-BBD}} = -5.08$ eV.[27,29] The redox potential for 4-PBD has not yet been reported, since it is not commercially available but rather synthesized in our own laboratory. However, its structure is similar to that of the 4-methoxybenzene diazonium salt, with a reported value of $E_{redox,4\text{-MBD}} = -4.87$ eV.[27,29] On the basis of eqs 1 and 2 and Figure 2, we thus expect a lower reaction rate for 4-PBD compared with 4-NBD and 4-BBD.

Role of Physical Structure

The chemical reactivity of graphene is influenced by its physical structure, including the number of layers, the type and structure of edges, the degree of strain and grain boundaries.

Layer Number Dependence. In our laboratory, we have studied the reactivity of graphene flakes of varying thicknesses under reaction, 17−25 mM 4-NBD in water with 1 wt % sodium dodecyl sulfate (SDS) at 35−45 °C for 7−12 h.[8] After functionalization, regions of single layer graphene (SLG) showed a much higher degree of reaction than the bilayer graphene (BLG) and multilayer graphene (MLG) regions, as indicated by the D peak intensity in the Raman spectra (Figure 3a).[8] The reaction rate as a function of time was measured by Koehler et al. and is seen to be significantly lower on the BLG than on the SLG (Figure 3d,e).[17]

Initially we supposed that the I_D/I_G variation was due to thicker graphene having more layers contributing to the G peak, with only the top reacted layer contributing to the D peak. This would result in a $1/N$ dependency of k_{ET}, but this relation does not fit the experimental data (Figure 3c). We also considered the different DOS for SLG, BLG, and MLG and its contribution to the reaction rate in the Gerischer−Marcus model; however, this trend also fails to describe the data (Figure 3c).[8]

A likely explanation is that charged impurities in the SiO_2 substrate induce electron and hole puddles in graphene, which are regions of 10−100 nm diameter where the local Dirac point is shifted above or below E_F, respectively. Based on the relative energy levels of graphene and the diazonium molecule (Figure 2), the reactivity is increased in n-doped puddles and suppressed in p-doped puddles. SLG on SiO_2 has been shown to have significant charge inhomogeneity with electron−hole puddles,[30] where the presence of electron puddles enhances reactivity. However, for BLG and MLG, the top layer where the reactions occur is screened from the charged impurities in the substrate by the underlying layers and thus does not experience the charge fluctuations that lead to regions of increased reactivity.[8]

Mechanical strain in the graphene lattice has been theoretically shown to increase chemical reactivity,[31] and

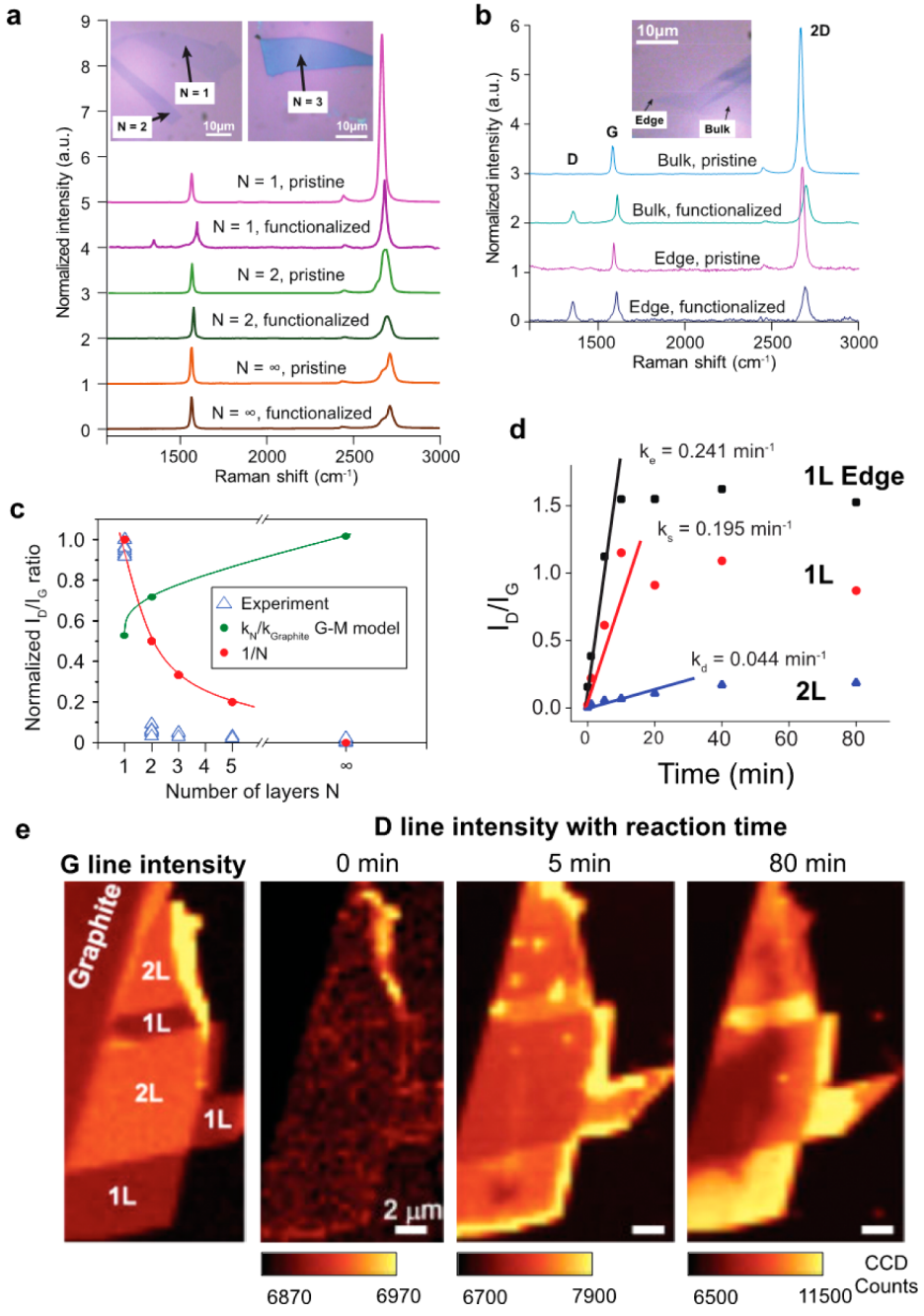

FIGURE 3. (a) Raman spectra before and after functionalization for SLG ($N = 1$), BLG ($N = 2$), and MLG ($N = \infty$). Inset shows optical images of mechanically exfoliated graphene flakes. (b) Raman spectra for SLG in bulk of flake and at edge. (c) Normalized I_D/I_G as a function of layer number N. (d) Reaction rates based on I_D/I_G for SLG (1L), BLG (2L), and SLG edges (1L Edge). (e) Spatial Raman maps showing evolution of D peak intensity with reaction time for a flake with SLG (1L) and BLG (2L) regions. Panels a–c adapted from ref 8. Copyright 2010 American Chemical Society. Panels d and e adapted from ref 17. Copyright 2010 John Wiley and Sons.

graphene is corrugated with nanometer-scale ripples.[32] The curvature helps to accommodate the movement of carbon atoms out of plane when changing from sp^2 to sp^3 hybridization upon covalent functionalization.[8,33] The top layer in BLG and MLG is expected to be flatter than SLG, since it is attached to the layers below and cushioned from the roughness of the SiO_2 substrate.

Edge Dependence. Edges have been theoretically shown to influence the chemical and physical properties of graphene.[5] In most samples, the edge structures are a mixture of armchair and zigzag regions (Figure 4a,d), dangling bonds, and other disordered structures. The disorder at graphene edges is observed as a polarization-dependent D peak in the Raman spectrum.[34] Zigzag edges have also been

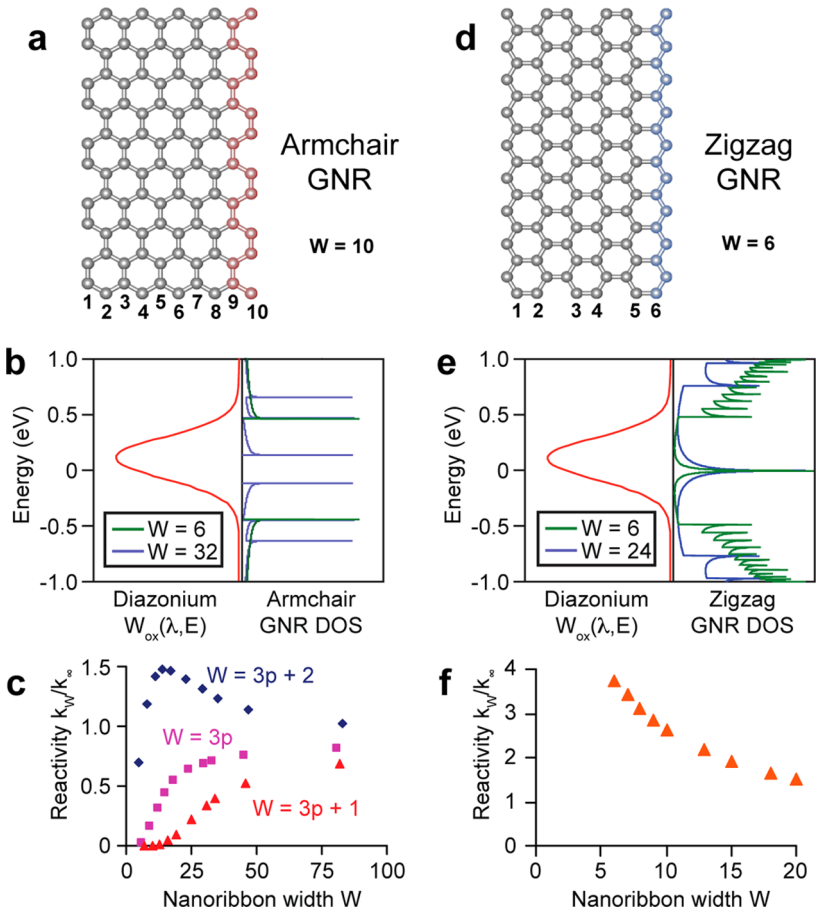

FIGURE 4. (a) Schematic of an armchair GNR with $W = 10$. (b) DOS vs energy diagram for armchair GNRs calculated by third-nearest-neighbor tight-binding for $W = 6$ (green lines) and 32 (blue lines) and DOS for the diazonium salt. (c) Electron transfer rate constants from Gerischer–Marcus theory as a function of the ribbon width W, normalized to a wide ribbon ($W = 83$). (d) Schematic of a zigzag GNR with width $W = 6$. (e) DOS vs energy diagram for zigzag GNRs for $W = 6$ (green lines) and 24 (blue lines), calculated by first-nearest-neighbor tight-binding within the Hückel approximation. (f) Relative reaction rate constants for zigzag GNRs from Gerischer–Marcus theory. Adapted from ref 9. Copyright 2009 American Chemical Society.

shown by STM and STS to have an increased density of states (DOS).[35] Due to the combined effect of the disordered atomic structures and enhanced DOS, an increased chemical reactivity is expected.

Raman spectra of the edges and interiors of the mechanically exfoliated flakes on SiO_2/Si before and after functionalization with 4-NBD are shown in Figure 3b (same reaction conditions as the layer-dependent study were used).[8] After functionalization, the increase in D peak intensity at the edge is much higher than that in the flake interior. Furthermore, the D peak intensity at the edge is no longer polarization-dependent, indicating that covalent functionalization dominates its intensity.[8]

Others have also reported enhanced reactivity at graphene edges.[17,18] In the time-resolved Raman study by Koehler et al. discussed above, the initial reaction rate of the edge was measured to be 1.2 times higher than that in the interior of the SLG flake under aqueous reaction conditions (Figure 3d).[17] Spatially and temporally resolved Raman mapping showed the reacted regions spreading from the edges toward the interior of the flake (Figure 3e). In addition, the increased reactivity has been partially attributed to the edge atoms more easily accommodating the strain of sp^2 bonds changing to sp^3.[17] An earlier report showed that the edges of highly oriented pyrolytic graphite (HOPG) are more reactive than the bulk and that glassy carbon (GC), a graphitic material containing many edges, is also more reactive.[36]

Graphene Nanoribbons. Graphene nanoribbons (GNRs) are narrow sheets of graphene where the carriers are quantum-confined in the transverse direction, which results in a band gap that is inversely dependent on the ribbon width.[37] Understanding the selectivity of the diazonium reaction for GNRs with different physical and electronic structures could enable strategies for separating and sorting them. The electronic, magnetic, and chemical properties of GNRs have been explored with extensive computational efforts, as summarized by Barone et al.[38]

In armchair GNRs (Figure 4a), the ribbon width of W atoms can be grouped into three families: $W = 3p$, $3p + 1$, and $3p + 2$, with p an integer. Combining the calculated band structures with Gerischer–Marcus theory (eqs 1 and 2), we calculated the electron transfer rate constant k_{ET} for each GNR family as a function of W and normalized it to that of a quasi-infinitely wide ribbon ($W = 83$). The overlap between the empty states of the diazonium salt and the GNR band structure is shown in Figure 4b. As shown in Figure 4c, k_{ET} increases for increasing W and saturates toward similar values for large W, with the reactivities of the different families being ranked as $k_{3p+2} > k_{3p} > k_{3p+1}$.[9] We performed a similar analysis for zigzag GNRs (Figure 4d–f),[9] which resulted in a higher overall reactivity, mostly due to the higher DOS of the center band. Moreover, k_{ET} decreases with increasing W since narrower ribbons have a larger contribution from the zigzag edges where there is localization of charge. First principles calculations have been used by Jiang et al. to show that both the localized edge states and the center band in the DOS are more readily functionalized by various radical groups.[39] These differences in reaction rates suggest it may be possible to selectively functionalize GNRs based on structure.[9] GNRs have been produced experimentally via both top-down and bottom-up approaches,[37,40] but the predicted reactivity trends have yet to be studied experimentally.

Grain Boundaries. Graphene grown by chemical vapor deposition (CVD) is polycrystalline with grain sizes ranging from ~0.1 to 100 μm, depending on growth conditions.[41] The grain boundaries (GBs) do not follow crystallographic orientations and are made up of carbon pentagons, heptagons, and distorted hexagons,[41] which lead to both compressive and tensile strain.[42] Theoretical calculations suggest an increased local DOS at GBs at zero energy,[42] which combined with the increased strain could increase chemical reactivity. Further work combining spectroscopy and atomically resolved imaging is needed to experimentally elucidate the role of GBs in graphene reactivity.

Role of Substrate

As an atomically thin layer, graphene is strongly influenced by its surroundings. Graphene is commonly deposited on SiO_2/Si wafers, which allows for its visual identification and for conventional lithographic device fabrication techniques. In recent years, the interface between graphene and its supporting substrate has been engineered to improve device performance by decreasing surface roughness, decreasing surface dipoles, screening the SiO_2 charged impurities from the graphene, and preventing the adsorption of dipolar impurities between the substrate and the graphene.[43] In order of increasing degree of improvement, these techniques include forming self-assembled monolayers (SAMs) on the substrate prior to depositing graphene,[15] using hexagonal boron nitride (hBN) as the substrate,[44] and making suspended graphene.[45]

Since the supporting substrate affects the local DOS of graphene, both its chemical and electronic properties are affected. We have studied the effect of four different substrates on the reactivity of CVD-grown graphene toward covalent 4-NBD functionalization.[10] Raman spectra of graphene on each substrate before and after functionalization are shown in Figure 5a. The reactivity of CVD graphene on bare SiO_2 and Al_2O_3 is relatively higher, leading to values of $I_D/I_G > 1$, while the reactivity on OTS and hBN is relatively lower, with I_D/I_G near 0.3.[10]

Analysis of the Raman spectra shows that the pristine graphene is slightly p-doped overall on OTS and hBN while being more highly p-doped on SiO_2 and Al_2O_3.[10] Furthermore, since the 2D peak position upshifts for p-doped graphene but downshifts for n-doped,[25] a sample with many p- and n-doped puddles that are smaller than the laser spot size would result in an inhomogeneously broadened 2D peak. We observe this for graphene on SiO_2 and Al_2O_3, while the 2D peak is narrower for OTS and hBN,[10] suggesting weaker charge puddles. This likely occurs because OTS and hBN increase the distance between the graphene sheet and the charged impurities in the SiO_2 and prevent the adsorption of polar impurities (e.g., water).[33] Graphene deposited on hexamethyldisilazane (HMDS)-coated SiO_2 also showed lower reactivity than on a bare SiO_2 surface.[33] These observations are consistent with the influence of substrate-induced electron–hole puddles and ripples on graphene reactivity, as described earlier.

The role of electron–hole puddles in these experiments was tested by modeling the reactivity using Gerischer–Marcus theory (eqs 1 and 2) and fitting it to the experimentally derived Fermi level data.[10] However, the average E_F determined from the value of I_{2D}/I_G and the 2D position does not fit the model predictions (Figure 6b). The schematic in Figure 6a illustrates that a sample with low overall p-doping and low electron–hole puddle amplitude (e.g., OTS, hBN) would have few n-doped, reactive regions. But a sample with higher overall p-doping but high puddle amplitude (e.g., SiO_2, Al_2O_3) would have many more n-doped regions for electron transfer. Once the experimental data is offset by the width of the 2D peak to account for puddles, they follow the model trend (Figure 6c).[10]

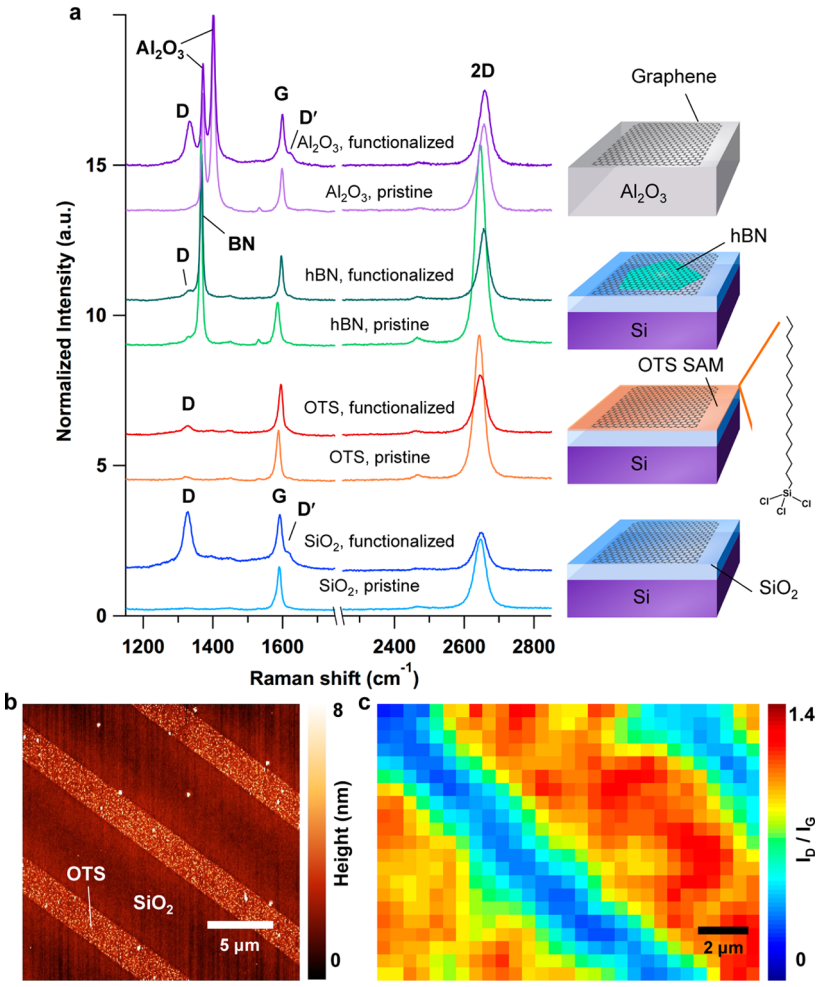

FIGURE 5. (a) Raman spectra for pristine and 4-NBD functionalized CVD graphene on four different substrates: SiO_2; octadecyltrichlorosilane (OTS) coated SiO_2; hexagonal boron nitride (hBN); sapphire (Al_2O_3). Reaction conditions: 10 mM 4-NBD in aqueous solution with 0.5 wt % SDS at 35 °C for 16 h. (b) Atomic force microscopy (AFM) image of OTS lines patterned on SiO_2. (c) Raman map of I_D/I_G for graphene on the patterned substrate after 4-NBD functionalization. Reaction conditions were the same as in part a but 1.5 h reaction time. Adapted from ref 10. Copyright 2012 Nature Publishing Group.

The high contrast in graphene reactivity for different substrates was exploited to pattern the graphene with a new technique called reactivity imprint lithography (RIL). The substrate is chemically patterned: we patterned SiO_2 with OTS lines by using a PDMS stamp (Figure 5b).[10] The portions of graphene resting on SiO_2 react strongly after 4-NBD functionalization, while the portions on OTS are only slightly functionalized, as shown by a mapping of I_D/I_G (Figure 5c).[10] This technique was also used to spatially pattern proteins onto graphene without using harsh conventional lithography steps that would otherwise damage the biomolecules.[10]

Applications of Covalent Functionalization

Tuning Electronic Properties. The conduction and valence bands in SLG touch each other at six distinct points in momentum space (called K-points), making it a zero-gap semiconductor. Opening a band gap is required for making transistors that can be effectively switched off. Methods that have been explored to achieve this include partial oxidation, reduction of graphene oxide, hydrogenation, fluorination, and chemical modification.[2,3,5,46] Diazonium modification appears promising, because it results in a significant increase of the room-temperature resistance,[11] an optical band gap of ~380 meV based on ARPES measurements,[12] and a defect-hopping related transport gap of ~80 meV in suspended, heavily functionalized graphene.[13] However, a 25% coverage in an ordered (1,4)-pattern is needed to open a useful band gap of ~2 eV,[23] and as discussed earlier, this has not yet been possible to achieve. We note that it has been theoretically shown that bilayer graphene that is functionalized on both sides has a larger band gap than bilayer that is only functionalized on one side.[47] However, a similar study for monolayer graphene has not been

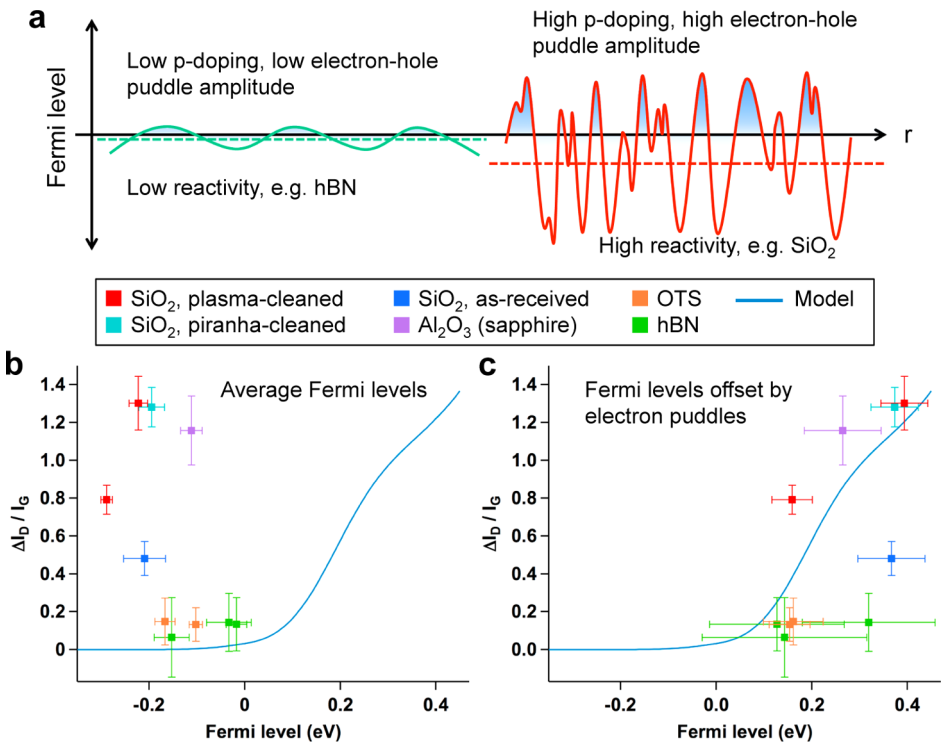

FIGURE 6. (a) Schematic illustration of spatial variation of graphene Fermi level, E_F (solid lines), and average E_F (dashed lines) on different substrates. (b) Change in I_D/I_G after 4-NBD reaction as a function of average E_F before reaction for graphene on various substrates (colored data points). Electron transfer model is shown in blue curve. (c) Initial E_F shifted to show E_F within n-doped puddles. Reproduced from ref 10. Copyright 2012 Nature Publishing Group.

published to the best of our knowledge. Further study is needed to elucidate the role of geometry and reaction conditions on band gap opening of functionalized graphene.

Control over doping levels and Fermi energy in graphene is required for many (opto-)electronic applications.[5,48] Graphene can be p-doped by the adsorption of electron-withdrawing groups to shift E_F below the Dirac point or n-doped by adsorption of electron-donating groups to shift it above.[5,20] In our laboratory, we have compared the effect of attaching diazonium salts with different functional groups (4-NBD, 4-BBD, and 4-PBD).[7] Histograms of I_D/I_G and I_{2D}/I_G for graphene reacted with these diazonium salts are shown in Figure 7a–c. I_D/I_G increases due to covalent functionalization, but the change is the least pronounced for 4-PBD, consistent with Gerisher–Marcus theory, as discussed earlier. Moreover, the propargyloxy-group is larger than the nitro- and bromo-groups (Figure 7d) and thus creates more steric hindrance. Finally, 4-PBD may also form more or longer oligomers that physisorb onto the graphene and block off reaction sites.

The I_{2D}/I_G ratio decreases for both p- and n-doping,[25] and here it decreases after all three types of functionalization, with the change being least pronounced for 4-PBD. It should be noted though that the difference in I_{2D}/I_G ratio between 4-PBD and the other two chemistries (4-NBD and 4-BBD) is less pronounced than the difference for the I_D/I_G ratio (Figure 7a-c). We consider two factors that decrease the 2D peak intensity after diazonium functionalization, as illustrated in Figure 7d. First, graphene loses an electron to reduce the diazonium salt to an aryl radical, so based on the change of I_D/I_G, this factor dominates for 4-NBD and 4-BBD. Second, physisorbed diazonium molecules and oligomers can dope the graphene via surface charge transfer, and based on its structure and the Raman data, we expect that this effect dominates for 4-PBD.

The charge transport characteristics of a graphene field effect transistor (FET) show the effect of chemistry on the electronic properties of graphene. The applied gate voltage, V_G, shifts the Fermi level, E_F, in the graphene channel, controlling its resistivity. Transfer curves of source–drain current as a function of V_G show a dip at the charge-neutrality point, where E_F passes through the Dirac point. P-type doping shifts the charge-neutrality point to positive V_G and n-type doping to negative V_G.[20] Farmer and co-workers have shown that long-range scatterers (due to physisorption) shift the charge-neutrality point and decrease the mobility of only one type of carrier: hole dopants reduce the electron mobility, whereas electron dopants reduce the

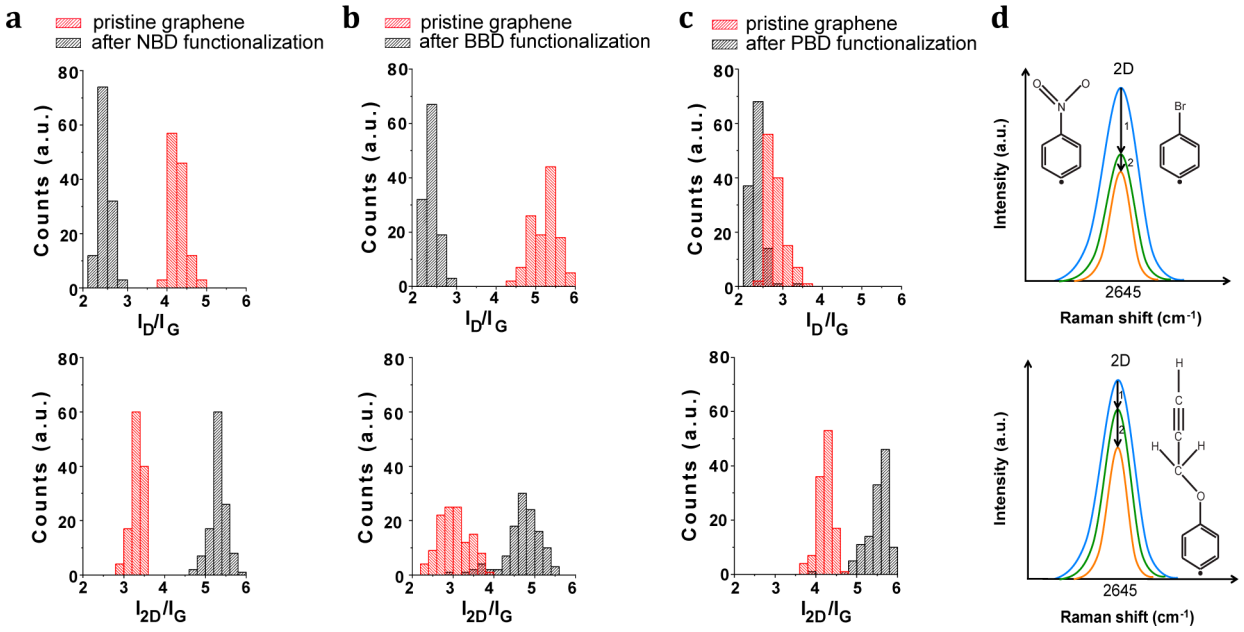

FIGURE 7. (a–c) Effect of different diazonium functional groups on Raman spectra of CVD-grown graphene. Reactions conditions: 10 mM aqueous solution with 1 wt % of SDS for 12 h at 35 °C. Raman spectroscopy was performed at 633 nm laser excitation. Top panels show I_D/I_G histograms and bottom panels I_{2D}/I_G histograms after functionalization with (a) 4-NBD, (b) 4-BBD, and (c) 4-PBD. (d) Schematic showing the 2D peak intensity decreases due to (1) loss of electrons due to covalent bond formation and (2) doping due to physisorbed species, and the relative amounts of these for 4-NBD and 4-BBD (top panel) compared with 4-PBD (bottom panel). Adapted from ref 10. Copyright 2012 Nature Publishing Group.

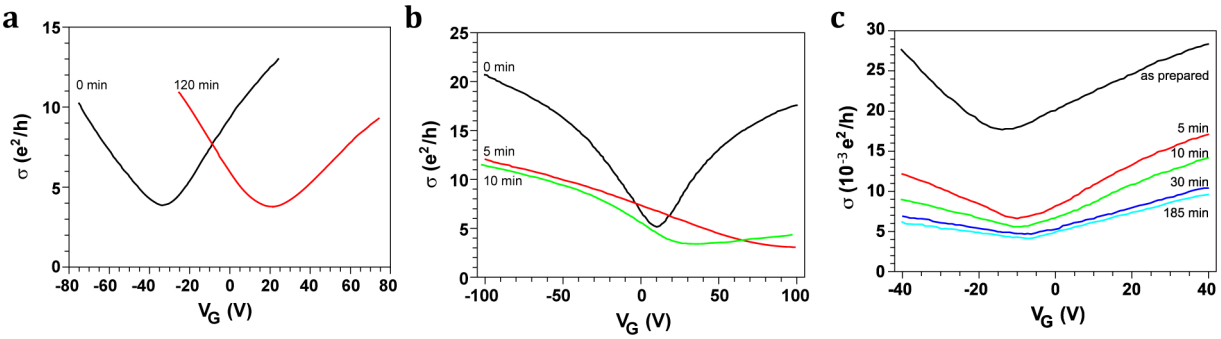

FIGURE 8. Effect of reaction conditions on the charge transport characteristics of graphene FETs: (a) 4-BBD (1 mM) in 1:1 water/methanol mixture at 300 K for 2 h. Adapted from ref 20. (b) 4-NBD (20 mM) in aqueous solution with 1 wt % SDS at 300 K for 5–10 min. Adapted from ref 21. (c) 4-NBD (4 mM) in acetonitrile at 300 K for 5–185 min at 300 K. Adapted from ref 14.

hole mobility.[20] Short-range scatterers (due to chemisorption) decrease the minimum conductivity and the mobility of both types of charge carriers.[20] Depending on the reaction conditions, graphene transistors exposed to diazonium salts can show the effects of both to different degrees: physisorption can be favored over chemisorption (Figure 8a),[20] both effects can be present in relatively equal degrees (Figure 8b),[21] or chemisorption can be dominant (Figure 8c).[14]

Composites, Biosensors and Catalysts. Graphene is a promising additive in polymer matrices for mechanical and electronic applications due to its high tensile strength, thermal and electrical conductivity, and low thermal expansion coefficient.[49] Graphene is biocompatible and can be coupled with proteins, bacteria, cells, and DNA and can act as a biosensor.[50] When graphene is coupled with nanoparticles, catalysts with a high specific area are formed.[51] Johnson and co-workers used a diazonium-based tether to attach photosensitive proteins on a graphene FET to achieve photocurrent switching.[52] Graphene-based composite and biosensing work is commonly done with graphite oxide (GO) due to its processability, water solubility, and reactivity with additional species.[53] However, its electronic properties are inferior to those of graphene, and it is chemically heterogeneous.

In our group, we have developed a technique to make water-soluble pristine graphene without the use of surfactants to stabilize the dispersion.[6] Solution-phase graphene

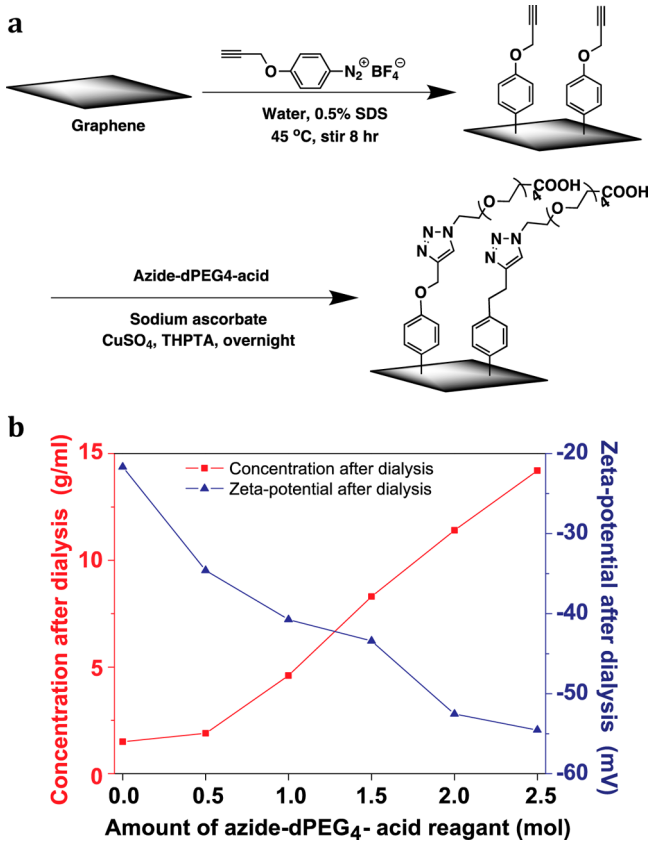

FIGURE 9. (a) Reaction scheme for the diazonium functionalization of graphene followed by click-chemistry with a PEG-COOH moiety. (b) Effect of azido-dPEG4-acid on colloidal stability of the click-functionalized solution-phase graphene. Adapted from ref 6. Copyright 2011 American Chemical Society.

was made by thermal expansion of intercalated graphite, followed by dispersion in a sodium cholate aqueous solution.[54] The solution-phase graphene was covalently functionalized with 4-PBD in the presence of SDS to provide a handle for click-chemistry attachment (via 1,3-dipolar azide–alkyne cycloaddition) of a short chain poly(ethylene glycol) (PEG) molecule terminated by a carboxylic acid, as illustrated in Figure 9a.[6] The click-functionalized graphene is stable after removal of the surfactant, as shown by surface tension and ζ potential measurements (Figure 9b).

Conclusions and Outlook

In this Account, we have reviewed the extensive literature focused on functionalizing graphene with diazonium salts. We covered the reaction mechanism both from a theoretical and from an experimental perspective and found that although thermodynamics predict long-range ordering, in reality the process is mostly governed by kinetics and influenced by electron–hole puddles and ripples. Depending on the reaction conditions, the entire range between physisorption and chemisorption can be achieved, as shown by Raman spectroscopy and charge transport characteristics of functionalized graphene transistors. The degree of reactivity is also strongly influenced by the structure of graphene: monolayers react more strongly than multilayers and edges are more prone to react than the basal plane of the graphene. We have also reviewed some applications of covalently functionalized graphene and discuss how its electronic properties can be modulated by means of different chemistries and reaction conditions. The functionalized graphene can be used as a biosensor, filler in polymeric matrices, and catalyst in solution. The diazonium chemistry is a versatile, convenient, and powerful tool for selectively modifying and manipulating graphene.

BIOGRAPHICAL INFORMATION

Geraldine L. C. Paulus obtained her B.S. and M.S. in chemical engineering from the Katholieke Universiteit Leuven (KUL) in Belgium. She is currently a Ph.D. candidate at the Massachusetts Institute of Technology (MIT), under the supervision of Professor Michael Strano. She works on the physics, chemistry, and engineering of low-dimensional carbon materials for energy and sensing applications.

Qing Hua Wang is a postdoctoral research associate in chemical engineering at the Massachusetts Institute of Technology (MIT). She received her B.A.Sc. in Engineering Science at the University of Toronto and her Ph.D. in Materials Science and Engineering at Northwestern University. Her research interests include self-assembly, graphene chemistry, and scanning probe microscopy.

Michael S. Strano is the Charles and Hilda Roddey Professor of Chemical Engineering at the Massachusetts Institute of Technology (MIT). His research focuses on biomolecule/nanoparticle interactions and the surface chemistry of low-dimensional systems, nanoelectronics, nanoparticle separations, and applications of vibrational spectroscopy to nanotechnology. Michael has received numerous awards for his work and was ranked among the top 20 chemists of the past decade by Thomson Reuters based on citation impact scores for chemistry publications. http://web.mit.edu/stranogroup/

FOOTNOTES

*E-mail address: strano@mit.edu.
The authors declare no competing financial interest.
†These authors contributed equally.

REFERENCES

1 Geim, A. K. Graphene: Status and prospects. *Science* **2009**, *324*, 1530–1534.
2 Loh, K. P.; Bao, Q.; Ang, P. K.; Yang, J. The chemistry of graphene. *J. Mater. Chem.* **2010**, *20*, 2277–2289.
3 Niyogi, S.; Bekyarova, E.; Hong, J.; Khizroev, S.; Berger, C.; de Heer, W.; Haddon, R. C. Covalent chemistry for graphene electronics. *J. Phys. Chem. Lett.* **2011**, *2*, 2487–2498.
4 Sun, Z.; James, D. K.; Tour, J. M. Graphene chemistry: Synthesis and manipulation. *J. Phys. Chem. Lett.* **2011**, *2*, 2425–2432.
5 Liu, H.; Liu, Y.; Zhu, D. Chemical doping of graphene. *J. Mater. Chem.* **2011**, *21*, 3335–3345.

6 Jin, Z.; McNicholas, T. P.; Shih, C.-J.; Wang, Q. H.; Paulus, G. L. C.; Hilmer, A.; Shimizu, S.; Strano, M. S. Click chemistry on solution-dispersed graphene and monolayer CVD graphene. *Chem. Mater.* **2011**, *23*, 3362–3370.

7 Paulus, G. L. C.; M.H., H.; Wang, Q. H.; Hilmer, A. J.; Kim, K. K.; Shih, C. J.; Ulissi, Z.; Kong, J.; Strano, M. S. Substituent Effects for the Control of Covalent Electronic Doping of CVD Graphene. 2012, manuscript in preparation.

8 Sharma, R.; Baik, J. H.; Perera, C. J.; Strano, M. S. Anomalously large reactivity of single graphene layers and edges toward electron transfer chemistries. *Nano Lett.* **2010**, *10*, 398–405.

9 Sharma, R.; Nair, N.; Strano, M. S. Structure-reactivity relationships for graphene nanoribbons. *J. Phys. Chem. C* **2009**, *113*, 14771–14777.

10 Wang, Q. H.; Jin, Z.; Kim, K. K.; Hilmer, A. J.; Paulus, G. L. C.; Shih, C.-J.; Ham, M.-H.; Sanchez-Yamagishi, J. D.; Watanabe, K.; Taniguchi, T.; Kong, J.; Jarillo-Herrero, P.; Strano, M. S. S. Understanding and controlling the substrate effect on graphene electron transfer chemistry via reactivity imprint lithography. *Nat. Chem.* **2012**, *4*, 724–732.

11 Bekyarova, E.; Itkis, M. E.; Ramesh, P.; Berger, C.; Sprinkle, M.; de Heer, W. A.; Haddon, R. C. Chemical modification of epitaxial graphene: Spontaneous grafting of aryl groups. *J. Am. Chem. Soc.* **2009**, *131*, 1336–1337.

12 Niyogi, S.; Bekyarova, E.; Itkis, M. E.; Zhang, H.; Shepperd, K.; Hicks, J.; Sprinkle, M.; Berger, C.; Lau, C. N.; Deheer, W. A.; Conrad, E. H.; Haddon, R. C. Spectroscopy of covalently functionalized graphene. *Nano Lett.* **2010**, *10*, 4061–4066.

13 Zhang, H.; Bekyarova, E.; Huang, J.-W.; Zhao, Z.; Bao, W.; Wang, F.; Haddon, R. C.; Lau, C. N. Aryl functionalization as a route to band gap engineering in single layer graphene devices. *Nano Lett.* **2011**, *11*, 4047–4051.

14 Sinitskii, A.; Dimiev, A.; Corley, D. A.; Fursina, A. A.; Kosynkin, D. V.; Tour, J. M. Kinetics of diazonium functionalization of chemically converted graphene nanoribbons. *ACS Nano* **2010**, *4*, 1949–1954.

15 Yan, Z.; Sun, Z.; Lu, W.; Yao, J.; Zhu, Y.; Tour, J. M. Controlled modulation of electronic properties of graphene by self-assembled monolayers on SiO_2 substrates. *ACS Nano* **2011**, *5*, 1535–1540.

16 Hossain, M. Z.; Walsh, M. A.; Hersam, M. C. Scanning tunneling microscopy, spectroscopy, and nanolithography of epitaxial graphene chemically modified with aryl moieties. *J. Am. Chem. Soc.* **2010**, *132*, 15399–15403.

17 Koehler, F. M.; Jacobsen, A.; Ensslin, K.; Stampfer, C.; Stark, W. J. Selective chemical modification of graphene surfaces: Distinction between single and bilayer graphene. *Small* **2010**, *6*, 1125–1130.

18 Lim, H.; Lee, J. S.; Shin, H.-J.; Shin, H. S.; Choi, H. C. Spatially resolved spontaneous reactivity of diazonium salt on edge and basal plane of graphene without surfactant and its doping effect. *Langmuir* **2010**, *26*, 12278–12284.

19 Englert, J. M.; Dotzer, C.; Yang, G.; Schmid, M.; Papp, C.; Gottfried, J. M.; Steinrueck, H.-P.; Spiecker, E.; Hauke, F.; Hirsch, A. Covalent bulk functionalization of graphene. *Nat. Chem.* **2011**, *3*, 279–286.

20 Farmer, D. B.; Golizadeh-Mojarad, R.; Perebeinos, V.; Lin, Y.-M.; Tulevski, G. S.; Tsang, J. C.; Avouris, P. Chemical doping and electron-hole conduction asymmetry in graphene devices. *Nano Lett.* **2009**, *9*, 388–392.

21 Fan, X.-Y.; Nouchi, R.; Yin, L.-C.; Tanigaki, K. Effects of electron-transfer chemical modification on the electrical characteristics of graphene. *Nanotechnology* **2010**, *21*, No. 475208.

22 Jiang, D.-E.; Sumpter, B. G.; Dai, S. How do aryl groups attach to a graphene sheet? *J. Phys. Chem. B* **2006**, *110*, 23628–23632.

23 Boukhvalov, D.; Katsnelson, M. Tuning the gap in bilayer graphene using chemical functionalization: Density functional calculations. *Phys. Rev. B* **2008**, *78*, No. 085413.

24 Zhu, H.; Huang, P.; Jing, L.; Zuo, T.; Zhao, Y.; Gao, X. Microstructure evolution of diazonium functionalized graphene: A potential approach to change graphene electronic structure. *J. Mater. Chem.* **2012**, *22*, 2063–2068.

25 Das, A.; Pisana, S.; Chakraborty, B.; Piscanec, S.; Saha, S.; Waghmare, U.; Novoselov, K.; Krishnamurthy, H.; Geim, A.; Ferrari, A. Monitoring dopants by Raman scattering in an electrochemically top-gated graphene transistor. *Nat. Nanotechnol.* **2008**, *3*, 210–215.

26 Bard, A. J.; Faulkner, L. R. *Electrochemical Methods: Fundamentals and Applications* Wiley: New York, 1980; Vol. 2.

27 Nair, N.; Kim, W.-J.; Usrey, M. L.; Strano, M. S. A structure−reactivity relationship for single walled carbon nanotubes reacting with 4-hydroxybenzene diazonium salt. *J. Am. Chem. Soc.* **2007**, *129*, 3946–3954.

28 Barone, V.; Peralta, J. E.; Uddin, J.; Scuseria, G. E. Screened exchange hybrid density-functional study of the work function of pristine and doped single-walled carbon nanotubes. *J. Chem. Phys.* **2006**, *124*, No. 024709.

29 Elofson, R. M.; Gadallah, F. Substituent effects in the polarography of aromatic diazonium salts. *J. Org. Chem.* **1969**, *34*, 854–857.

30 Martin, J.; Akerman, N.; Ulbricht, G.; Lohmann, T.; Smet, J. H.; von Klitzing, K.; Yacoby, A. Observation of electron-hole puddles in graphene using a scanning single-electron transistor. *Nat. Phys.* **2008**, *4*, 144–148.

31 De Andres, P. L.; Vergés, J. A. First-principles calculation of the effect of stress on the chemical activity of graphene. *Appl. Phys. Lett.* **2008**, *93*, No. 171915.

32 Fasolino, A.; Los, J. H.; Katsnelson, M. I. Intrinsic ripples in graphene. *Nat. Mater.* **2007**, *6*, 858–861.

33 Fan, X.; Nouchi, R.; Tanigaki, K. Effect of charge puddles and ripples on the chemical reactivity of single layer graphene supported by SiO_2/Si substrate. *J. Phys. Chem. C* **2011**, *115*, 12960–12964.

34 Casiraghi, C.; Hartschuh, A.; Qian, H.; Piscanec, S.; Georgi, C.; Fasoli, A.; Novoselov, K. S.; Basko, D. M.; Ferrari, A. C. Raman spectroscopy of graphene edges. *Nano Lett.* **2009**, *9*, 1433–1441.

35 Tao, C.; Jiao, L.; Yazyev, O. V.; Chen, Y.-C.; Feng, J.; Zhang, X.; Capaz, R. B.; Tour, J. M.; Zettl, A.; Louie, S. G.; Dai, H.; Crommie, M. F. Spatially resolving edge states of chiral graphene nanoribbons. *Nat. Phys.* **2011**, *7*, 616–620.

36 Liu, Y.-C.; McCreery, R. L. Reactions of organic monolayers on carbon surfaces observed with unenhanced Raman spectroscopy. *J. Am. Chem. Soc.* **1995**, *117*, 11254–11259.

37 Dutta, S.; Pati, S. K. Novel properties of graphene nanoribbons: A review. *J. Mater. Chem.* **2010**, *20*, 8207–8223.

38 Barone, V.; Hod, O.; Peralta, J. E.; Scuseria, G. E. Accurate prediction of the electronic properties of low-dimensional graphene derivatives using a screened hybrid density functional. *Acc. Chem. Res.* **2011**, *44*, 269–279.

39 Jiang, D.-e.; Sumpter, B. G.; Dai, S. Unique chemical reactivity of a graphene nanoribbon's zigzag edge. *J. Chem. Phys.* **2007**, *126*, No. 134701.

40 Jia, X.; Campos-Delgado, J.; Terrones, M.; Meunier, V.; Dresselhaus, M. S. Graphene edges: A review of their fabrication and characterization. *Nanoscale* **2011**, *3*, 86–95.

41 Huang, P. Y.; Ruiz-Vargas, C. S.; van der Zande, A. M.; Whitney, W. S.; Levendorf, M. P.; Kevek, J. W.; Garg, S.; Alden, J. S.; Hustedt, C. J.; Zhu, Y.; Park, J.; McEuen, P. L.; Muller, D. A. Grains and grain boundaries in single-layer graphene atomic patchwork quilts. *Nature* **2011**, *469*, 389–392.

42 Wang, B.; Puzyrev, Y.; Pantelides, S. T. Strain enhanced defect reactivity at grain boundaries in polycrystalline graphene. *Carbon* **2011**, *49*, 3983–3988.

43 Lafkioti, M.; Krauss, B.; Lohmann, T.; Zschieschang, U.; Klauk, H.; Klitzing, K. v.; Smet, J. H. Graphene on a hydrophobic substrate: Doping reduction and hysteresis suppression under ambient conditions. *Nano Lett.* **2010**, *10*, 1149–1153.

44 Dean, C. R.; Young, A. F.; Meric, I.; Lee, C.; Wang, L.; Sorgenfrei, S.; Watanabe, K.; Taniguchi, T.; Kim, P.; Shepard, K. L.; Hone, J. Boron nitride substrates for high-quality graphene electronics. *Nat. Nanotechnol.* **2010**, *5*, 722–726.

45 Du, X.; Skachko, I.; Barker, A.; Andrei, E. Y. Approaching ballistic transport in suspended graphene. *Nat. Nanotechnol.* **2008**, *3*, 491–495.

46 Schwierz, F. Graphene transistors. *Nat. Nanotechnol.* **2010**, *5*, 487–496.

47 Yuan, L.; Li, Z.; Yang, J.; Hou, J. Diamondization of chemically functionalized graphene and graphene-BN bilayers. *Phys. Chem. Chem. Phys.* **2012**, *14*, 8179–8184.

48 Wehling, T. O.; Novoselov, K. S.; Morozov, S. V.; Vdovin, E. E.; Katsnelson, M. I.; Geim, A. K.; Lichtenstein, A. I. Molecular doping of graphene. *Nano Lett.* **2007**, *8*, 173–177.

49 Kuilla, T.; Bhadra, S.; Yao, D.; Kim, N. H.; Bose, S.; Lee, J. H. Recent advances in graphene based polymer composites. *Prog. Polym. Sci.* **2010**, *35*, 1350–1375.

50 Mohanty, N.; Berry, V. Graphene-based single-bacterium resolution biodevice and DNA transistor: interfacing graphene derivatives with nanoscale and microscale biocomponents. *Nano Lett.* **2008**, *8*, 4469–4476.

51 Scheuermann, G. M.; Rumi, L.; Steurer, P.; Bannwarth, W.; Mülhaupt, R. Palladium nanoparticles on graphite oxide and its functionalized graphene derivatives as highly active catalysts for the Suzuki−Miyaura coupling reaction. *J. Am. Chem. Soc.* **2009**, *131*, 8262–8270.

52 Lu, Y.; Lerner, M. B.; Qi, Z. J.; Mitala, J. J. J.; Lim, J. H.; Discher, B. M.; Johnson, A. T. C. Graphene-protein bioelectronic devices with wavelength-dependent photoresponse. *Appl. Phys. Lett.* **2012**, *100*, No. 033110.

53 Compton, O. C.; Nguyen, S. T. Graphene oxide, highly reduced graphene oxide, and graphene: Versatile building blocks for carbon-based materials. *Small* **2010**, *6*, 711–723.

54 Shih, C.-J.; Vijayaraghavan, A.; Krishnan, R.; Sharma, R.; Han, J.-H.; Ham, M.-H.; Jin, Z.; Lin, S.; Paulus, G. L. C.; Reuel, N. F.; Wang, Q. H.; Blankschtein, D.; Strano, M. S. Bi- and trilayer graphene solutions. *Nat. Nanotechnol.* **2011**, *6*, 439–445.